IEEE Journal of Microwaves

Received 20 July 2022; revised 27 August 2022; accepted 29 August 2022. Date of publication 23 September 2022; date of current version 7 October 2022.

Digital Object Identifier 10.1109/JMW.2022.3204801

Modelization Methodology for the Quality Factor of Quarter-Wavelength n-Section Coaxial Stepped Impedance Resonators

JESSICA BENEDICTO (Member, IEEE), JEAN-FRANÇOIS FAVENNEC (Member, IEEE), ALEJANDRO BUITRAGO BERNAL, AND ERIC RIUS (Senior Member, IEEE)

(Regular Paper)

Lab-STICC UMR CNRS 6285, 29238 Brest, France

CORRESPONDING AUTHOR: Jessica Benedicto (e-mail: jessica.benedicto@univ-brest.fr).

This work did not involve human subjects or animals in its research.

ABSTRACT This paper proposes a method to develop an analytical model and/or numerical resolution of the quality factor of quarter-wavelength n-section coaxial stepped impedance resonators (SIRs). The topology is based on cascaded coaxial sections nested within each other. Thanks to the SIR effect, this type of geometrical arrangement offers practical degrees of freedom to modulate the size of the resonator in both longitudinal and transverse dimensions. Moreover, in an air-filled configuration, it provides interesting quality factor, although this depends on its shape factor at any given frequency. In this paper, we show the added value of using an analytical model or numerical resolution for the quality factor, to be able to optimize the topology. To demonstrate the advantages of this model and the numerical method, comparisons of two- and three-section coaxial SIRs at two different frequencies are proposed and discussed. To validate the analytical model and numerical resolution, the values are compared with ones obtained in eigenmodes *ANSYS HFSS* with electromagnetic simulation tool.

INDEX TERMS Analytical model, coaxial resonator, numerical resolution, quality factor, stepped impedance resonator.

I. INTRODUCTION

There is a continually growing need for small-sized microwave filters with good electrical performances: insertion losses, amplitude flatness, phase linearity, wide band rejection, and power handling. In terms of manufacturing, low sensitivity and low cost are also highly valued. For transmission filters operating at high power, volumic technologies, based, for example, on cylindrical or rectangular resonators are required [1], [2]. Such topologies also offer a very high quality factor, which can be easily calculated using well-known formulas. Although they do not eliminate the electromagnetic simulation of the filter, these analytical formulas are very useful to quickly design a filter that best meets a given specification. Although these solutions are often used in C, Ku, or Ka bands, they are not well suited for lower frequency bands for which the wavelengths are much larger. For example, at low frequencies, when the required quality factor is a few thousand, other less cumbersome topologies, such as coaxial ones [3], may be preferentially used. One of the main advantages of the coaxial waveguide or resonator is that it can support TEM mode, which means that it can be considered as a transmission line. In terms of filter design, this has significant advantages. Moreover, due to its particular geometric construction, there is an exact analytical formula for the quality factor. This configuration offers a degree of freedom enabling the best values to be chosen by adjusting the transverse dimensions. The length or the longitudinal dimension of a coaxial resonator is conditioned by the working frequency, the dielectric permittivity of the possible filling material, and of the chosen quarter- or half-wavelength configuration. Obviously, when high quality factors are required, the resonators are filled with air. To adjust to specific size constraints, it is necessary to modulate the dimensions of the structure. For the longitudinal dimensions, a very convenient

solution is to use a stepped impedance configuration. The ultimate of these consists in nesting the different sections of the coaxial resonator. This solution has the advantage of combining the nesting effect, i.e., a division of the length by the number of sections, and the SIR effect. Another advantage is the number of degrees of freedom associated with the number of interleaved sections, which allows the positions of the transmission zeros and harmonic frequencies to be adjusted with respect to the fundamental frequency. However, the arrangement of the coaxial sections has an impact on the value of the quality factor, for which there is no model.

Many studies on the modeling of TEM resonators, implemented in different topologies, are available in the literature. For instance, [4] presents the expression of the quality factor of a quarter-wavelength coaxial resonator. After proposing the topology of SIR coaxial resonators and their use in filters, Yamashita, Makimoto et al. and Giovanni et al. developed models of their quality factor [5], [6], [7], [8]. However, they did not consider nested coaxial sections, and the number of sections was limited to two. Some other studies on coaxial SIR filters based on multi-layer printed-circuit board (PCB) technology also present interesting information on the quality factors of these resonators, but without models [9].

The aim of this paper is to propose a method to develop an analytical model and/or numerical resolution of the quality factor of nested two- and three-section coaxial stepped impedance resonators.

II. PRESENTATION OF THE STRUCTURE

The structure is a quarter-wavelength resonator, filled with a material with relative permittivity ε_{r_i}. It is composed of n coaxial sections consisting of $n+1$ cylinders (Fig. 1(a) and (b)). Each section is fitted inside another on the same level. From an electrical point of view, the equivalent model can be seen in Fig. 1(c) as a succession of coaxial sections in cascade, where the ground conductor of one section is the central core of the next, and vice versa. The coupling of one TEM coaxial section to the adjacent one is done at their open-end extremities, through coupling areas of lengths l_c, assumed to be small compared with the section lengths l_i. It is represented electrically by an ideal transformer with a ratio of -1. This study was conducted assuming weak discontinuities. In this case, the lengths l_i of each section are assumed to be identical with a length equal to l. For each section i, the external and internal diameters are defined by D_i and d_i. The propagation constant is represented by $\gamma_i = \alpha_i + j\beta_i$, where α_i and β_i are the attenuation and phase constants of section i, respectively. Under these conditions, the electrical length θ_i and characteristic impedance Z_i of the coaxial section are defined by:

$$\theta_i = \beta_i \, l \tag{1}$$

$$Z_i = \frac{1}{2\,\pi}\sqrt{\frac{\mu_0}{\varepsilon_0\,\varepsilon_{r_i}}}\,ln\left(\frac{D_i}{d_i}\right) \tag{2}$$

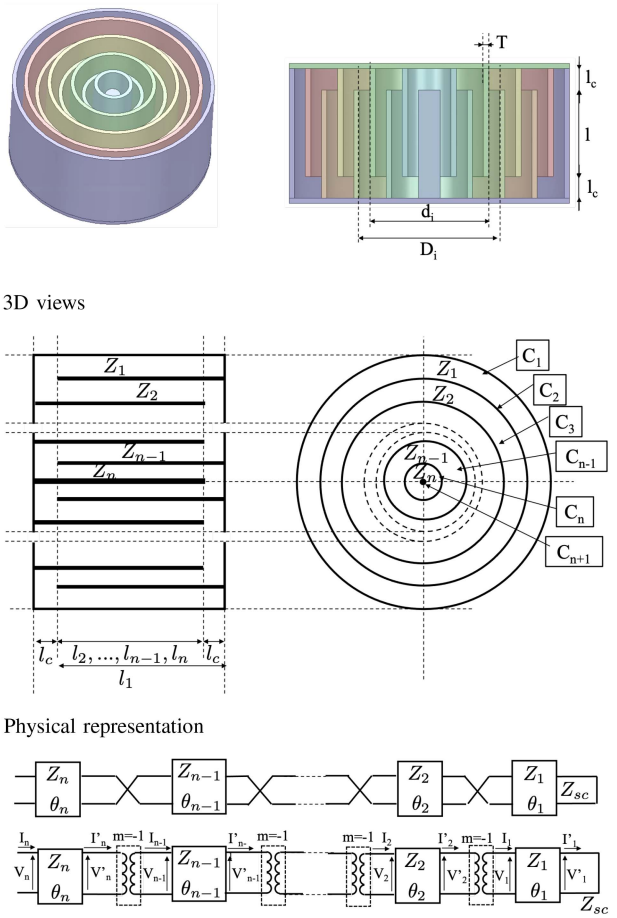

FIGURE 1. n-section coaxial SIR.

where ε_0 and μ_0 are vacuum permittivity and permeability, respectively. For this study, the dielectric is air so $\varepsilon_{r_i} = 1$.

The SIR effect, which is defined by M_{ij}, depends on the ratio of the characteristic impedances Z_i and Z_j of two adjacent coaxial TEM sections:

$$M_{i,i+1} = \frac{Z_i}{Z_{i+1}} \tag{3}$$

III. NUMERICAL RESOLUTION

A. GENERALITIES

Fig. 2(a) represents the equivalent circuit of a section of index i. A piece of line of infinitesimal length Δ_z can be modeled as a lumped-element circuit (Fig. 2(b)) where voltage and current are defined by:

$$u_i(z) = A_i\, e^{-\gamma_i\, z} + B_i\, e^{\gamma_i\, z} \tag{4}$$

$$i_i(z) = \frac{1}{Z_i}(A_i\, e^{-\gamma_i\, z} - B_i\, e^{\gamma_i\, z}) \tag{5}$$

where, A_i and B_i are complex amplitudes:

$$\begin{cases} A_i = A_i' + j\,A_i'', \\ B_i = B_i' + j\,B_i'' \end{cases} \tag{6}$$

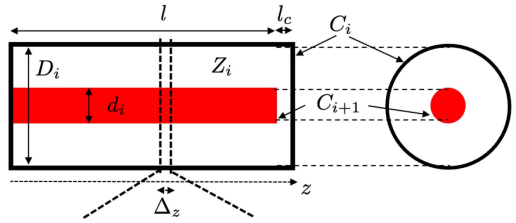

(a) Representation of a transmission line of index i

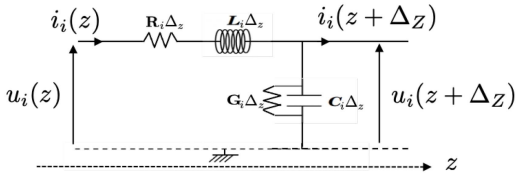

(b) Lumped-element equivalent circuit

FIGURE 2. Equivalent circuit for an infinitesimal length of transmission line.

In the lumped-circuit element (Fig. 2(b)), R and L are the series resistance and the inductance per unit length (in $\Omega.\mathrm{m}^{-1}$ and $H.\mathrm{m}^{-1}$), respectively, and G and C are the shunt conductance and the capacitance per-unit-length (in $S.\mathrm{m}^{-1}$ and $F.\mathrm{m}^{-1}$), respectively. The shunt conductance G is due to dielectric losses in the material between the conductors. In this structure, as the dielectric is air, the parameter G is zero. The terms σ, f_0, and ω_0 represent the conductivity of the metal, the fundamental frequency of the quarter-wavelength coaxial SIR, and the fundamental pulsation, respectively. The other quantities defined, at the fundamental frequency, for each section are:

$$\begin{cases} L_i = \frac{\mu_0}{2\pi}\, ln\left(\frac{D_i}{d_i}\right), \\ C_i = \frac{2\pi\varepsilon_0}{ln\left(\frac{D_i}{d_i}\right)}, \\ R_i = \frac{R_s}{2\pi}\left(\frac{2}{D_i}+\frac{2}{d_i}\right), \\ \gamma_i = \sqrt{j\,\omega_0\, C_i\ (R_i + \ j\,\omega_0\, L_i)}, \\ \alpha_i = \Re(\gamma_i), \\ \beta_i = \Im(\gamma_i) \end{cases} \tag{7}$$

where R_s is the surface resistance defined by:

$$Rs = \sqrt{\frac{\omega_0\,\mu_0}{2\,\sigma}} \tag{8}$$

The quality factor Q of a resonator can be defined, at the fundamental frequency, by the ratio between the average stored energy and the energy loss per second, multiplied by the fundamental pulsation.

For a coaxial SIR, the average stored energy can be defined as the sum of the average stored energy E_s^i of each line i, and the energy loss per second is the sum of the energy loss per second P_{tot}^i of each line i [6].

The quality factor of a coaxial SIR is defined by:

$$Q = \omega_0\, \frac{\sum_{i=1}^{n} E_s^i}{\sum_{i=1}^{n} P_{tot}^i} \tag{9}$$

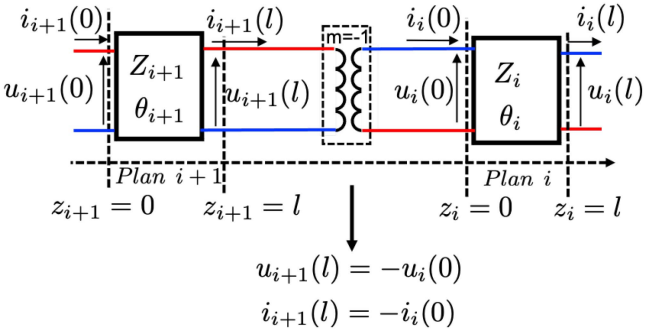

FIGURE 3. Transmission line continuity.

The average stored energy of each line E_s^i is the sum of the stored magnetic and electric energies, and can be defined in terms of voltage and current by:

$$\begin{aligned} E_s^i &= \int_0^l \left(\frac{1}{2}C_i < u_i(z)^2 > + \frac{1}{2}L_i < i_i(z)^2 >\right) dz \\ &= \frac{1}{4}\int_0^l \left[C_i\,(\Re(u_i(z)^2) + \Im(u_i(z)^2)) \right. \\ &\qquad \left. + L_i(\Re(i_i(z)^2) + \Im(i_i(z)^2))\right] dz \end{aligned} \tag{10}$$

where $< u_i(z)^2 >$ and $< i_i(z)^2 >$, as defined by (11), are the time average value of the square of the voltage and current at a fixed abscissa z.

$$< f(x) >= \frac{1}{2}(\Re(f(x)) + \Im(f(x))) \tag{11}$$

The energy loss per second of each line P_{tot}^i, represents the sum of the energy loss by joule effect in all the line P_l^i, and the energy loss in the short circuit P_{sc}^i:

$$\begin{aligned} P_l^i &= \int_0^l R_i < i_i(z)^2 > dz \\ &= \frac{1}{2}R_i \int_0^l (\Re(i_i(z)^2) + \Im(i_i(z)^2))dz \end{aligned} \tag{12}$$

$$\begin{aligned} P_{sc}^i &= \frac{1}{2}\int_{\frac{d_i}{2}}^{\frac{D_i}{2}} \frac{Rs}{2\pi\, r} < i_i(z=0\ or\ l)^2 > dr \\ &= \frac{1}{2}\frac{Rs}{2\pi} < i_i(z=0\ or\ l)^2 > \ln(D_i/d_i) \end{aligned} \tag{13}$$

B. RESONATOR ANALYSIS

1) CONTINUITY CONDITIONS

The continuity conditions between transmission lines are represented in Fig. 3. The coupling of one TEM coaxial section to the adjacent one is represented electrically by an ideal transformer with a ratio of -1. The continuity of currents and voltages from one section to another between each line can be formalized mathematically using the ideal transformer ABCD matrix:

$$\begin{pmatrix} u_{i+1}(l) \\ i_{i+1}(l) \end{pmatrix} = \begin{pmatrix} -1 & 0 \\ 0 & -1 \end{pmatrix} \begin{pmatrix} u_i(0) \\ i_i(0) \end{pmatrix} \tag{14}$$

Consequently, the voltage (or the current, respectively) at the end of the line at a length $z_{i+1} = l$ of the section Z_{i+1}, will be the opposite of the voltage (or the current, respectively) at the beginning of the line, i.e., $z_i = 0$, of the section Z_i. This condition is easily written as a system:

$$\begin{cases} u_{i+1}(l) = -u_i(0), \\ i_{i+1}(l) = -i_i(0) \end{cases} \tag{15}$$

By combining the system (15), with the (4) and (5), the amplitudes A_{i+1} and B_{i+1} can be written as functions of the amplitudes A_i and B_i:

$$\begin{cases} A_{i+1} = -\frac{1}{2}\, e^{\gamma_{i+1} l} \left(A_i + B_i + \frac{1}{M_{i,i+1}} (A_i - B_i) \right), \\ B_{i+1} = -\frac{1}{2}\, e^{-\gamma_{i+1} l} \left(A_i + B_i - \frac{1}{M_{i,i+1}} (A_i - B_i) \right) \end{cases} \tag{16}$$

2) INITIAL CONDITIONS

It is possible to distinguish two initial conditions.

The first of these concerns the section Z_1, which fixes the relation between the pair of amplitudes (A_1, B_1) and the length of the resonator $B_1 = f_1(A_1, l)$. This condition corresponds to the termination of the first section at the end of the line $(z_1 = l)$. If this termination is a short circuit as in this topology, the condition is $u_1(l) = 0$, so $B_1 = -A_1\, e^{-2\gamma_1 l}$. This first pair allows us to determine the set of amplitude pairs of each line as a function of the length l and the different coefficients M_{ij}, using the system (16): $(A_2, B_2) = f_2(A_1, \gamma_2, l, M_{12})$,.... $(A_n, B_n) = f_n(A_1, l, M_{12}, \gamma_i, \ldots, M_{n-1,n})$.

The second condition concerns the last section Z_n, at the beginning of the line at $z_n = 0$. This study offers the possibility to treat the open circuit case $i_n(0) = 0$, which results in a relation between the pair of amplitudes A_n and B_n:

$$A_n = B_n \tag{17}$$

Previous studies [10], [11], and [12] consider an approximation of low losses dedicated to high Q. These papers have shown that it is possible to define an identical relation for a quarter-wavelength coaxial SIR, regardless of the number of sections, which at the fundamental frequency links the electrical length $\theta = \beta\, l$ of each section of the resonator to the equivalent impedance ratio M_{ns}:

$$\tan(\beta\, l) = \frac{1}{\sqrt{M_{ns}}} \tag{18}$$

M_{ns} is defined as an equivalent impedance ratio that depends only on the coefficients M_{ij}, and whose formulation is different according to the number of sections n. For example, the expressions of the equivalent impedance ratios for two and three-section resonators are ([11], [12]), respectively:

$$\begin{cases} M_{2\,s} = M_{12}, \\ M_{3\,s} = M_{12} + M_{23} + M_{12} M_{23} \end{cases} \tag{19}$$

For more simplicity, the equivalent impedance ratio M_{ns} will be noted M whatever the number of sections.

In the approximation of low losses, after development, the relation (17) correspond to the relation (18). The method described in this paper [12] to determine the value of the equivalent impedance ratio is generalizable to a number of sections greater than 3, and can be done numerically using Matlab software.

The relation (18) allows us to determine the length l of each section of the resonator for a fixed fundamental frequency and equivalent impedance ratio.

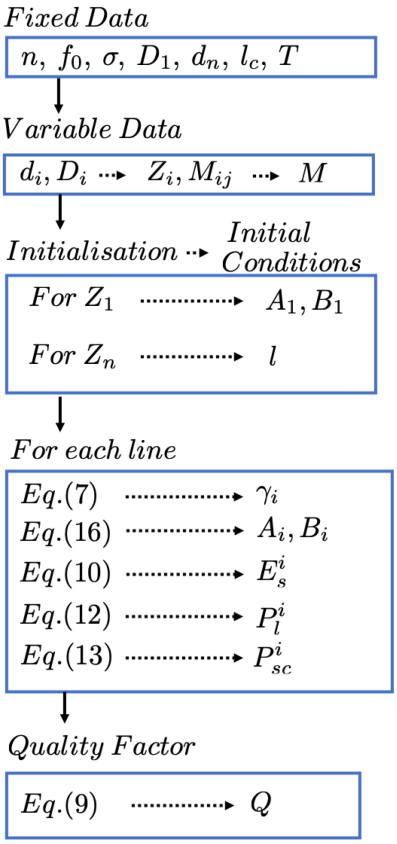

FIGURE 4. Principle of numerical resolution.

C. PRINCIPLE OF THE NUMERICAL RESOLUTION

Fig. 4 shows the principle of the numerical resolution developed with Matlab software. The first step, *"Data"*, consists in determining the geometrical dimensions of the resonator. It is of course possible to generate diameters in a totally random way, in order to directly calculate the quality factor of an isolated structure. However, for filters for which the fundamental frequency is fixed and the size is often a constraint, it is sometimes necessary to work at a constant footprint, by fixing the external section D_1.

Thus, the input parameters are the fundamental frequency f_0, the number of sections n, the electrical conductivity of the metal σ, and some geometrical quantities such as the external diameter of the first section D_1 (Fig. 1), the internal diameter of the n^{th} section d_n, the length of the discontinuity l_c, and the thickness of each cylinder T. Therefore, a numerical resolution in Matlab software makes it possible to generate, depending on the number of sections, the set of possible

diameters (D_i, d_i) of the whole structure, which more specifically fixes a set of possible characteristic impedances Z_i and all the coefficients M_{ij}. A numerical resolution based on ABCD matrix cascading and polynomial resolution is then used to calculate the equivalent impedance ratio M.

The second step is to define the initial conditions for the first and n^{th} sections. This step generates a relation between the complex amplitudes B_1 and A_1, and sets the length l of the resonators.

The third step computes the set of parameters γ_i and complex amplitudes A_i and B_i for each line, using the system (7) and continuity conditions (16). These expressions of the complex amplitudes A_i and B_i allow to calculate (for each section) the integrals of the time average value of the square of the voltage and current ($< u_i(z)^2 >$ and $< i_i(z)^2 >$) on the length of the coaxial line. Equations (10), (12), (13) allow us to calculate the stored and lost energies in each line.

Finally, the last step gives the value of the quality factor for several cases with fixed volume and fundamental frequency.

IV. ANALYTICAL MODELING

A. EXAMPLE OF A THREE-SECTION COAXIAL RESONATOR

The analytical modeling corresponds to the analytical development of the previous procedure, which can quickly become very cumbersome. For this reason, only the cases of two- and three-section resonators are studied in this section. Furthermore, we will show that the two-section case can be seen as a specific case of the three-section resonator. So, the three-section resonator case is presented first.

For this development, it is necessary to consider an approximation of low losses dedicated to high Q. In this case, the coefficient α_i is supposedly very low ($\alpha_i \ll 1$) and the following hypotheses are validated:

$$e^{2\,\alpha_i\,l} - 1 \approx 2\,\alpha_i\,l \tag{20}$$

$$1 - e^{-2\,\alpha_i\,l} \approx 2\,\alpha_i\,l \tag{21}$$

$$\gamma_i \approx j\frac{2\,\pi\,f_0}{c} \approx\ j\,\beta \approx \gamma \tag{22}$$

1) INITIAL CONDITIONS

The first line of the resonator is a transmission line with characteristic impedance Z_1 and a terminal short circuit, which implies:

$$u_1(l) = A_1\,e^{-\gamma\,l} + B_1\,e^{\gamma\,l} = 0 \tag{23}$$

This condition allows us to express the complex fraction $\frac{B_1}{A_1}$:

$$\frac{B_1}{A_1} = -\,e^{-2\gamma\,l} \tag{24}$$

The last line of the resonator is a transmission line with characteristic impedance Z_n and a terminal open circuit, which implies:

$$i_3(0) = \frac{1}{Z_3}(A_3\ - B_3) = 0 \Rightarrow B_3 = A_3 \tag{25}$$

2) COMPLEX AMPLITUDES

First, it is necessary to express the amplitudes (A_i, B_i) of each section in terms of the complex amplitudes A_1 and B_1 referring to (16). Then, for each expression, the first initial condition (24) enables us to replace the fraction $\frac{B_1}{A_1}$ by $-\,e^{-2\gamma\,l}$. After development, the complex amplitudes A_2, B_2, A_3, and B_3 of the second and third sections are:

$$A_2 = -\frac{1}{2}\,A_1\,e^{\gamma\,l}\left(1 -\ e^{-2\gamma\,l} + \frac{1}{M_{12}}(1 +\ e^{-2\gamma\,l})\right) \tag{26}$$

$$B_2 = -\frac{1}{2}\,A_1\,e^{-\gamma\,l}\left(1 -\ e^{-2\gamma\,l} - \frac{1}{M_{12}}(1 +\ e^{-2\gamma\,l})\right) \tag{27}$$

$$\begin{aligned} A_3 = \frac{A_1}{2}\,e^{\gamma\,l}\Bigg[&\cosh(\gamma\,l)\left((1 -\ e^{-2\gamma\,l}) + \frac{1 +\ e^{-2\gamma\,l}}{M_{23}M_{12}}\right) \\ &+ \sinh(\gamma\,l)\left(\frac{1}{M_{12}}(1 +\ e^{-2\gamma\,l}) + \frac{1}{M_{23}}(1 -\ e^{-2\gamma\,l})\right)\Bigg] \end{aligned} \tag{28}$$

$$\begin{aligned} B_3 = \frac{A_1}{2}\,e^{-\gamma\,l}\Bigg[&\cosh(\gamma\,l)\left((1 -\ e^{-2\gamma\,l}) - \frac{1 +\ e^{-2\gamma\,l}}{M_{12}M_{23}}\right) \\ &+ \sinh(\gamma\,l)\left(\frac{1}{M_{12}}(1 +\ e^{-2\gamma\,l}) - \frac{1}{M_{23}}(1 -\ e^{-2\gamma\,l})\right)\Bigg] \end{aligned} \tag{29}$$

By combining expressions (28) and (29) of the complex amplitudes A_3 and B_3, with the condition (25), we obtain the relation of a quarter-wavelength three-section coaxial SIR:

$$\begin{aligned} &\frac{1}{M_{23}M_{12}}\cosh^2(\gamma\,l) + \frac{1}{M_{23}}\sinh^2(\gamma\,l) \\ &\quad + \left(1 + \frac{1}{M_{12}}\right)\sinh(\gamma\,l)\cosh(\gamma\,l) \\ &\quad = e^{-2\gamma\,l}\left(-\frac{1}{M_{23}M_{12}}\cosh^2(\gamma\,l)\right. \\ &\quad \left. -\frac{1}{M_{23}}\sinh^2(\gamma\,l) + \left(1 + \frac{1}{M_{12}}\right)\sinh(\gamma\,l)\cosh(\gamma\,l)\right) \end{aligned} \tag{30}$$

Using trigonometric properties, and the low loss assumptions (22), this expression is simplified to become:

$$\tan^2(\beta\,l) = \frac{1}{M_{12} + M_{23} + M_{12}M_{23}} = \frac{1}{M} \tag{31}$$

The second part of the relation corresponds to the inverse of the equivalent impedance ratio M for a three-section resonator (19), defined in our previous study [12] and validating the relation (18).

This last relation allows us to express the set of complex amplitudes in terms of equivalent impedance ratio. For this, it

is necessary to use the following trigonometric equivalences.

$$\begin{cases} \cos(\beta\, l) = \cos\left(\arctan\left(\frac{1}{\sqrt{M}}\right)\right) = \sqrt{\frac{M}{M+1}}, \\ \sin(\beta\, l) = \sin\left(\arctan\left(\frac{1}{\sqrt{M}}\right)\right) = \sqrt{\frac{1}{M+1}}, \\ \cos(2\beta\, l) = \cos\left(2\,\arctan\left(\frac{1}{\sqrt{M}}\right)\right) = \frac{M-1}{M+1}, \\ \sin(2\beta\, l) = \sin\left(2\,\arctan\left(\frac{1}{\sqrt{M}}\right)\right) = \frac{2\sqrt{M}}{M+1} \end{cases} \tag{32}$$

All the complex amplitudes are now defined in the system (33).

$$\begin{cases} B_1 = A_1\left(-\frac{M-1}{M+1} + j\,\frac{2\sqrt{M}}{M+1}\right), \\ A_2 = -A_1\frac{1}{\sqrt{M+1}}\left(\frac{\sqrt{M}}{M_{12}} + j\right), \\ B_2 = -A_1\frac{\sqrt{M}(2\,M_{12}-M+1)+j\,(M_{12}(M-1)+2\,M)}{M_{12}(M+1)\sqrt{M+1}}, \\ A_3 = B_3 = A_1\,\frac{1}{M+1}\left(1+\frac{1}{M_{12}}\right)(1+j\,\sqrt{M}) \end{cases} \tag{33}$$

3) STORED AND LOST ENERGIES

By using the trigonometric properties (32), and the low loss approximation (20) and (21), the average stored energy and the energy loss per second P_l^i of each line can be expressed in terms of complex amplitudes and equivalent impedance ratio.

$$\begin{aligned} E_s^i &= \frac{1}{2}C_i\left(|A_i|^2\frac{1-e^{-2\,\alpha_i\,l}}{2\,\alpha_i} + |B_i|^2\frac{e^{2\,\alpha_i\,l}-1}{2\,\alpha_i}\right) \\ &= \frac{1}{2}C_i\left(|A_i|^2+|B_i|^2\right)\,l \end{aligned} \tag{34}$$

$$\begin{aligned} P_l^i = \frac{1}{2}\frac{R_i}{Z_i^2}\Bigg(&|A_i|^2\frac{1-e^{-2\,\alpha_i\,l}}{2\,\alpha_i} + |B_i|^2\frac{e^{2\,\alpha_i\,l}-1}{2\,\alpha_i} \\ &- 2(A_i'\,B_i' + A_i''\,B_i'')\frac{\sin(2\beta\,l)}{2\,\beta} \\ &+ 2(A_i''\,B_i' - A_i'\,B_i'')\frac{\cos(2\beta\,l)-1}{2\,\beta}\Bigg) \\ = \frac{1}{2}\frac{R_i}{Z_i^2}\Bigg[&\left(|A_i|^2+|B_i|^2\right)\,l \\ &- \frac{2}{(M+1)\,\beta}\Big[(A_i''\,B_i' - A_i'\,B_i'') \\ &+\sqrt{M}(A_i'\,B_i' + A_i''\,B_i'')\Big]\Bigg] \end{aligned} \tag{35}$$

For the energy loss in the short circuits, we distinguish two cases. The first is P_{sc}^1, which corresponds to the short circuit of the first section at $z_1 = l$, and all the other short circuits P_{sc}^i, which are systematically placed at the beginning of the line at $z_i = 0$. In the case of the three-section resonator, there are three cases of short circuit, which are represented on Fig. 6.

$$P_{sc}^1 = \frac{1}{2\,Z_1^2}\frac{R_s}{2\pi}\ln\frac{D_1}{d_1}4|A_1|^2 \tag{36}$$

For i different from 1:

$$P_{sc}^i = \frac{1}{2\,Z_i^2}\frac{R_s}{2\pi}\ln\frac{D_{i-1}}{d_i}\left[|A_i|^2+|B_i|^2-2(A_i'\,B_i' + A_i''\,B_i'')\right] \tag{37}$$

4) QUALITY FACTOR

For a three-section resonator, the quality factor results from all the different energies and powers stated above.

$$Q = \omega_0\,\frac{E_s^1+E_s^2+E_s^3}{P_l^1+P_l^2+P_l^3+P_{sc}^1+P_{sc}^2+P_{sc}^3} \tag{38}$$

Using the expressions (33) to (37), the quality factor can be presented in the following form:

$$\begin{aligned} Q = 2\,\omega_0\,\sqrt{\varepsilon_0\,\mu_0}\,M\,(M_{12}+1)/ \\ \Bigg[\frac{R_1}{Z_1}M_{12}(M+1) + \frac{R_2}{Z_2}(M_{12}^2+M) + \frac{R_3}{Z_3}M_{23}(M_{12}+1)^2 \\ + \frac{\sqrt{M}}{\arctan\left(\frac{1}{\sqrt{M}}\right)(M+1)}\Bigg(\frac{R_1}{Z_1}M_{12}(M+1) \\ - \frac{R_2}{Z_2}(M_{12}(M_{12}+2)-M) - \frac{R_3}{Z_3}M_{23}(M_{12}+1)^2\Bigg) \\ + \frac{2\,Rs\,\beta}{\arctan\left(\frac{1}{\sqrt{M}}\right)}\sqrt{\frac{\varepsilon_0}{\mu_0}}M_{12}(M+1)\Bigg(1+\frac{M}{M+1}\left(\frac{M_{12}+1}{M_{12}}\right) \\ + \frac{(M-M_{12})^2}{M_{12}(M+1)^2}\left(\frac{M_{23}+1}{M_{23}}\right)\Bigg)\Bigg] \end{aligned} \tag{39}$$

B. TWO-SECTION RESONATOR

It is possible to view the case of the two-section resonator as a specific case of three-section resonator by deleting all the terms M_{23}.

With this condition, the equivalent impedance ratio becomes $M = M_{12}$ and the quality factor is:

$$\begin{aligned} Q = 2\,\omega_0\,\sqrt{\varepsilon_0\,\mu_0}/ \\ \Bigg[\frac{R_1}{Z_1} + \frac{R_2}{Z_2} + \frac{\sqrt{M}}{\arctan\left(\frac{1}{\sqrt{M}}\right)(M+1)}\left(\frac{R_1}{Z_1} - \frac{R_2}{Z_2}\right) \\ + \frac{4\,Rs\,\beta}{\arctan\left(\frac{1}{\sqrt{M}}\right)}\sqrt{\frac{\varepsilon_0}{\mu_0}}\Bigg] \end{aligned} \tag{40}$$

This expression is the same as the one we should obtain by the procedure in the Section IV-A, from the expression of the quality factor for a two-section resonator :

$$Q = \omega_0\,\frac{E_s^1+E_s^2}{P_l^1+P_l^2+P_{sc}^1+P_{sc}^2} \tag{41}$$

V. VALIDATION OF MODELS

To validate the analytical and numerical resolution, we compared four different cases of resonators: two sets of two-section resonators at 150 MHz and 1.5 GHz, and two sets of three-section resonators at 150 MHz and 1.5 GHz.

For all cases, the external section D_1 is fixed at 30 mm, the internal diameter of the n^{th} section d_n at 2 mm, the coupling length l_c at 1 mm, the thickness of each cylinder T at 0.5 mm, and the metal is silver with a conductivity of 61 MS.m^{-1}.

TABLE 1. Comparison of Analytical Model and Electromagnetic Simulations of Two-Section Coaxial SIRs at 150 MHz

	D_1	d_1	D_2	d_2	l_{HFSS}	Z_1	Z_2	Q	Q	Δ
M	mm	mm	mm	mm	mm	Ω	Ω	$HFSS^{TM}$	$Analytic$	%
0.18		20.00	19.00		371.20	0.18	0.98	804	857	6.5
0.36		15.00	14.00		327.80	0.30	0.85	951	1000	5.2
0.54	30	12.00	11.00	2	297.80	0.40	0.74	991	1030	4.0
1.06		8.00	7.00		245.10	0.57	0.54	937	984	5.0
1.76		6.00	5.00		205.20	0.70	0.40	863	901	4.5
2.58		5.00	4.00		176.60	0.78	0.30	801	833	4.0
4.97		4.00	3.00		133.90	0.88	0.18	713	738	3.5

TABLE 2. Comparison of Analytical Model and Electromagnetic Simulations of Two-Section Coaxial SIRs at 1.5 GHz

	D_1	d_1	D_2	d_2	l_{HFSS}	Z_1	Z_2	Q	Q	Δ
M	mm	mm	mm	mm	mm	Ω	Ω	$HFSS^{TM}$	$Analytic$	%
0.20		9.64	9.14		29.20	0.19	0.96	2417	2510	3.9
0.45		6.64	6.14		25.10	0.35	0.79	2966	2800	5.6
1.24		3.64	3.14		16.70	0.62	0.50	2719	2541	6.5
3.06		2.34	1.84		14.50	0.81	0.26	2209	2071	6.3
4.65	30	2.04	1.54	2	12.53	0.87	0.19	2013	1880	6.6
7.23		1.84	1.34		10.30	0.91	0.13	1833	1709	6.8
10.14		1.74	1.24		8.70	0.94	0.09	1725	1596	7.5
17.28		1.64	1.14		6.50	0.96	0.06	1591	1439	9.6

TABLE 3. Comparison of Analytical Model and Electromagnetic Simulations of Three-Section Coaxial SIRs at 150 MHz

	D_1	d_1	D_2	d_2	D_3	d_3	l_{HFSS}	Z_1	Z_2	Z_3	M_{12}	M_{23}	Q	Q	Δ
M/FM	mm	mm	mm	mm	mm	mm	mm	Ω	Ω	Ω			$HFSS^{TM}$	$Analytic$	%
1 / 0.14		24.72	23.72	18.63	17.63		250	0.08	0.11	0.95	0.80	0.11	475	495	4.2
1 / 1.07		22.79	21.79	10.95	9.95		250	0.12	0.30	0.70	0.40	0.43	700	730	4.3
1 / 3.33		24.83	23.83	9.26	8.26		250	0.08	0.41	0.62	0.20	0.67	688	715	3.9
3 / 0.11		13.90	12.90	9.10	8.10		166	0.33	0.15	0.61	2.20	0.25	888	924	4.1
3 / 4.64		18.19	17.19	4.92	3.92		166	0.22	0.54	0.29	0.40	1.86	680	699	2.8
3 / 11.67	30	22.27	21.27	4.79	3.79	2	166	0.13	0.65	0.28	0.20	2.33	656	682	4.0
10 / 0.01		12.73	11.73	10.71	9.71		97	0.37	0.04	0.69	9.40	0.06	897	929	3.6
10 / 0.05		6.75	5.75	4.67	3.67		97	0.65	0.09	0.26	7.20	0.34	775	796	2.7
10 / 0.15		6.32	5.32	3.94	2.94		97	0.68	0.13	0.17	5.20	0.77	646	663	2.6
10 / 0.58		6.94	5.94	3.64	2.64		97	0.64	0.21	0.12	3.00	1.75	547	563	2.9
10 / 3.33		9.88	8.88	3.52	2.52		97	0.48	0.40	0.10	1.20	4.00	525	537	2.4

In the case of the analytical model, the expression of the equivalent impedance ratio M is known with the relations (19). It is then interesting to compare the quality factor as a function of the equivalent impedance ratio M for a two-section resonator and the form factor FM, which is the fraction $\frac{M_{23}}{M_{12}}$ for a three-section resonator. It is important to note that the same equivalent impedance ratio M can correspond to several sets of M_{ij} for a resonator made of more than two sections. For the cases of two-section resonators, the quality factor is plotted directly as a function of the impedance ratio $M =$

TABLE 4. Comparison of Analytical Model and Electromagnetic Simulations of Three-Section Coaxial SIRs at 1.5 GHz

	D_1	d_1	D_2	d_2	D_3	d_3	l_{HFSS}	Z_1	Z_2	Z_3	M_{12}	M_{23}	Q	Q	Δ
M/FM	mm	mm	mm	mm	mm	mm	mm	Ω	Ω	Ω			$HFSS^{TM}$	$Analytic$	%
1 / 0.42		22.74	21.74	13.69	12.69		20.50	0.12	0.20	0.80	0.60	0.25	1837	1911	4.0
1 / 3.33		24.83	23.83	9.26	8.26		20.50	0.08	0.41	0.62	0.20	0.67	1979	1990	0.6
3 / 0.04		17.64	16.64	13.57	12.57		14.50	0.23	0.09	0.80	2.60	0.11	2060	2117	2.7
3 / 0.11		13.90	12.90	9.10	8.10		14.50	0.33	0.15	0.61	2.20	0.25	2314	2315	0.1
3 / 4.64	30	18.19	17.19	4.92	3.92	2	14.50	0.22	0.54	0.29	0.40	1.86	1939	1844	4.9
10 / 0.01		11.03	10.03	9.00	8.00		8.70	0.43	0.05	0.60	9.20	0.08	2094	2056	1.8
10 / 0.13		6.32	5.32	3.99	2.99		8.70	0.68	0.13	0.17	5.40	0.72	1736	1608	7.4
10 / 0.58		6.94	5.94	3.64	2.64		8.70	0.64	0.21	0.12	3.00	1.75	1554	1400	9.9
10 / 2.56		9.21	8.21	3.53	2.53		8.70	0.51	0.37	0.10	1.40	3.58	1512	1347	10.9
10 / 3.35		9.88	8.88	3.52	2.52		8.70	0.48	0.40	0.10	1.20	4.02	1510	1348	10.7

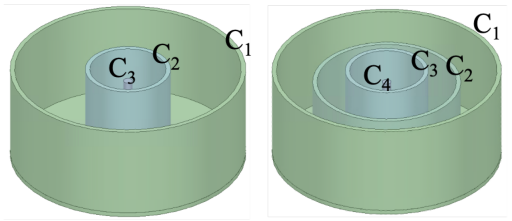

(a) 3D views

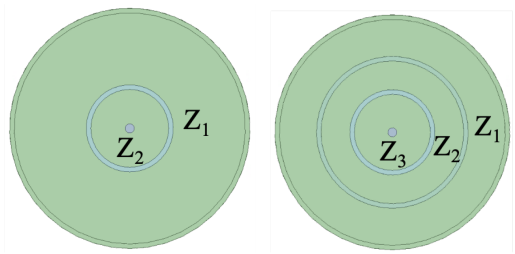

(b) Top cross-sections

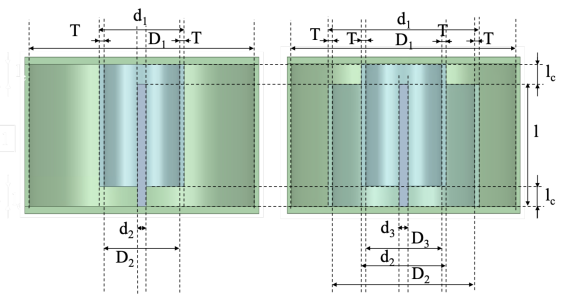

(c) Longitudinal cross-sections

FIGURE 5. Two- and three-section coaxial SIRs.

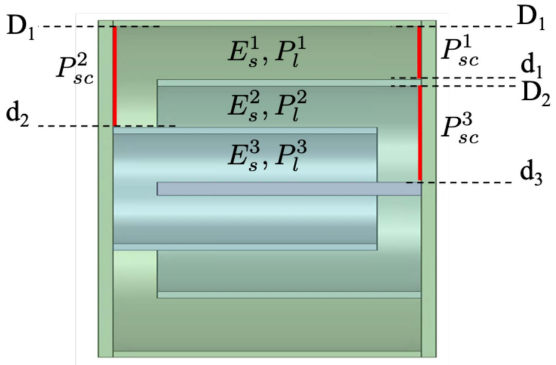

FIGURE 6. Position of short circuits in the case of a three-section resonator.

M_{12}. Conversely, for the cases of three-section resonators, the equivalent impedance ratio depends on the impedance ratios M_{12} and M_{23}, so there are several pairs (M_{12}, M_{23}) resulting from the same equivalent impedance ratio M. Therefore, to distinguish the different cases for the same M, the curve is plotted as a function of the form factor FM, which is the fraction $\frac{M_{23}}{M_{12}}$.

Tables 1 to 4 and Figs. 7 to 10 summarize all these cases. Each figure presents a comparison of the quality factor results obtained by numerical resolution or by analytical formula with those obtained by simulation in eigenmode of the resonator with the *ANSYS HFSS* electromagnetic simulation tool. All the figures show a good agreement between the values obtained by eigenmode simulation and the two models (analytical and numerical). In order to evaluate and compare the different possible configurations, a representation of the topologies for the most extreme cases and the theoretical length (obtained with (18)) of each resonator (dashed line) studied are plotted in Figs. 7 to 10.

The results of each simulation performed under *ANSYS HFSS* are listed in the tables and compared with the values of the quality factor obtained under the same conditions with the analytical formula. In addition, the relative difference between these two values is indicated in the last column of each table. First, the relative percentage difference never exceeds 11%, which allows the different models to be validated. Second, the comparisons show a better agreement

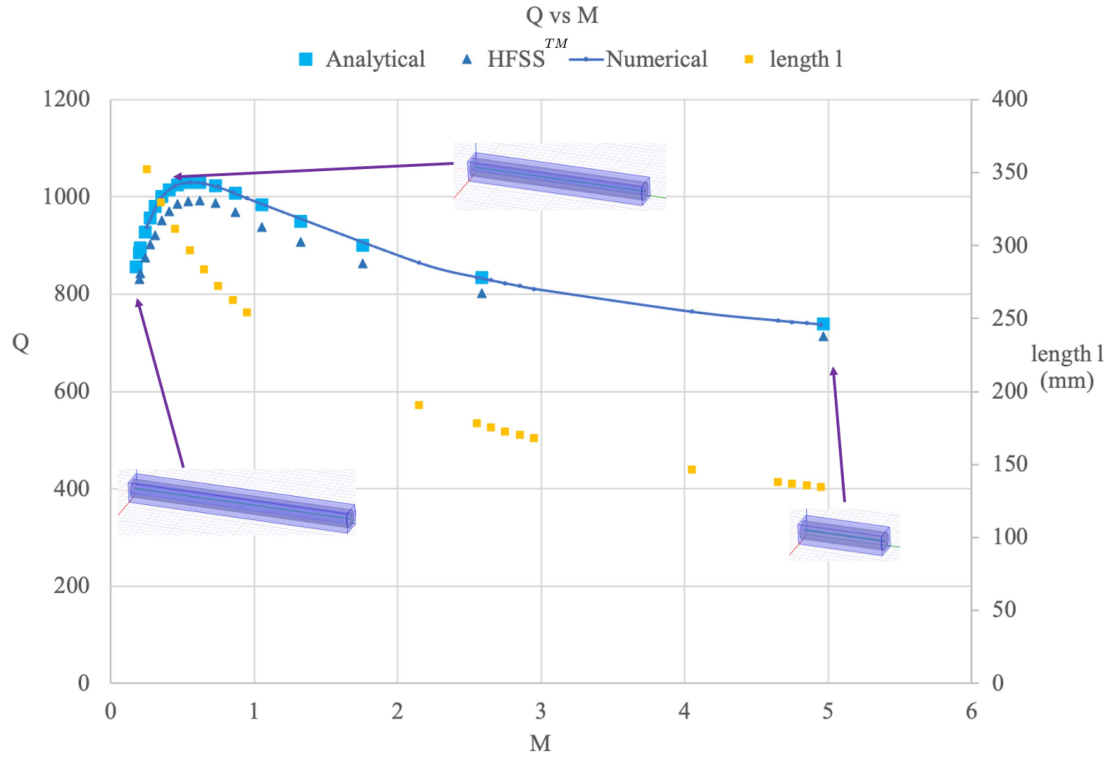

FIGURE 7. Quality factor vs. equivalent impedance ratio *M* for two-section coaxial SIRs at 150 MHz.

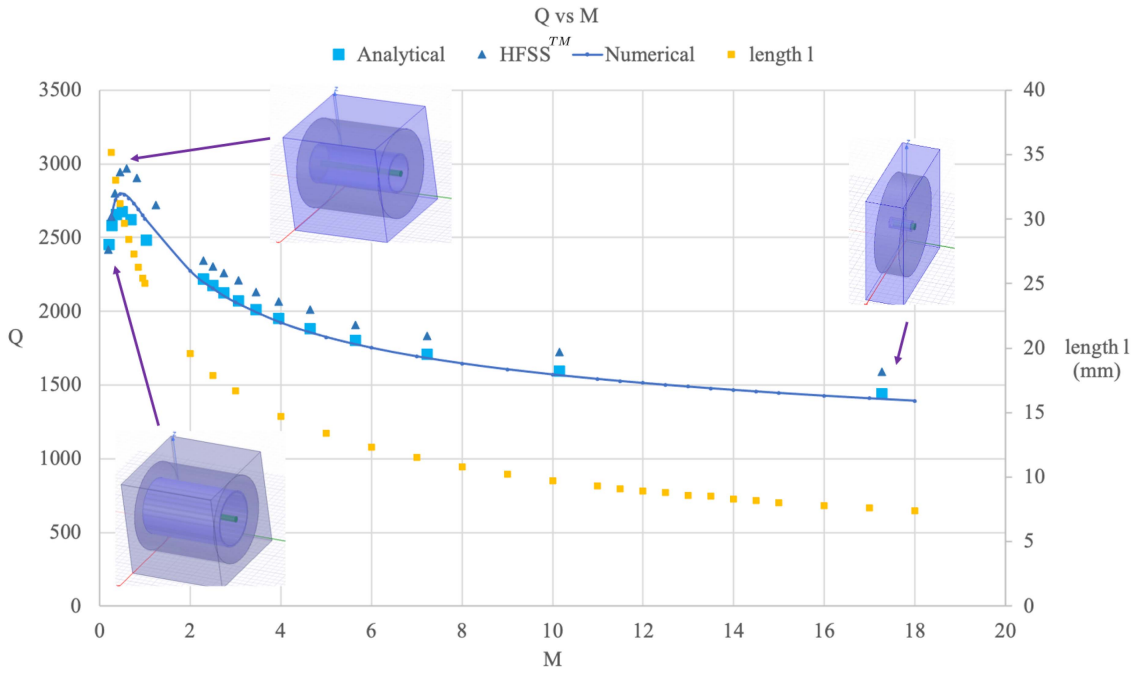

FIGURE 8. Quality factor vs. equivalent impedance ratio *M* for two-section coaxial SIRs at 1.5 GHz.

for the 150 MHz frequency than the 1.5 GHz case, whatever the number of sections. Finally, the two-section case shows smaller deviations than the three-section case. All these conclusions are due to discontinuity effects, mainly at the extremities. In fact, the case of the three-section resonator presents an additional discontinuity (Fig. 5(c)) compared with the two-section resonators, which explains the few notable differences between the results of the two topologies. At the same time, whereas the length l_c is fixed at 1 mm in all cases, the length of the resonators is 10 times greater for those at

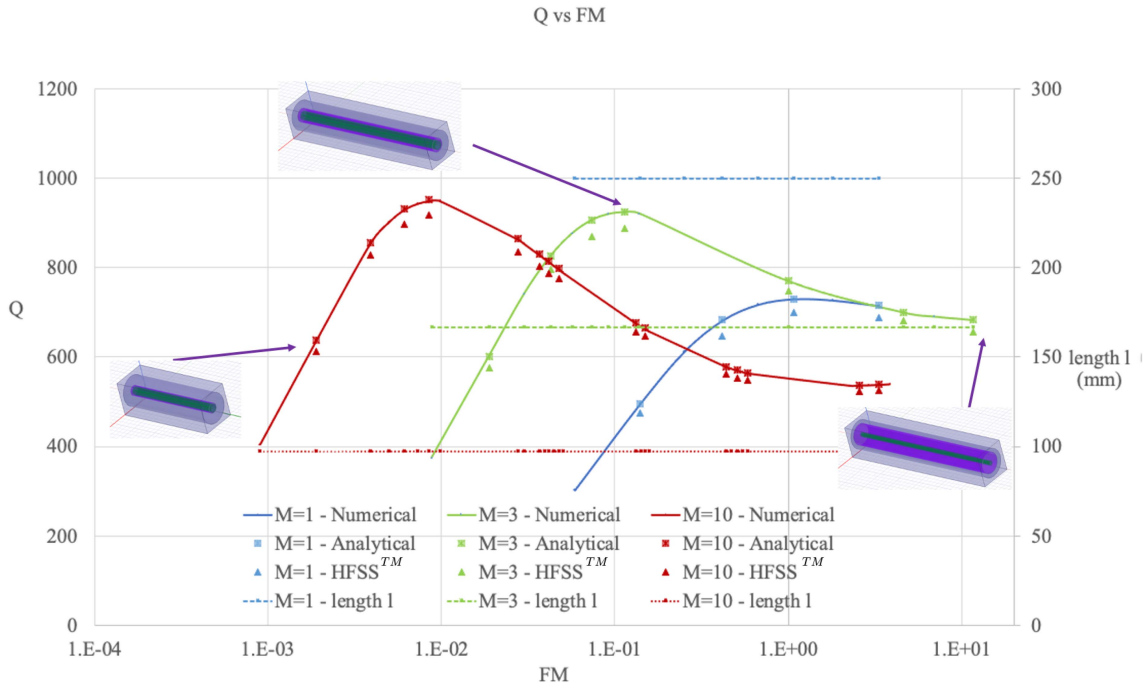

FIGURE 9. Quality factor vs. logarithm of factor FM for equivalent impedance ratios equal to 1, 3, and 10 for three-section coaxial SIRs at 150 MHz.

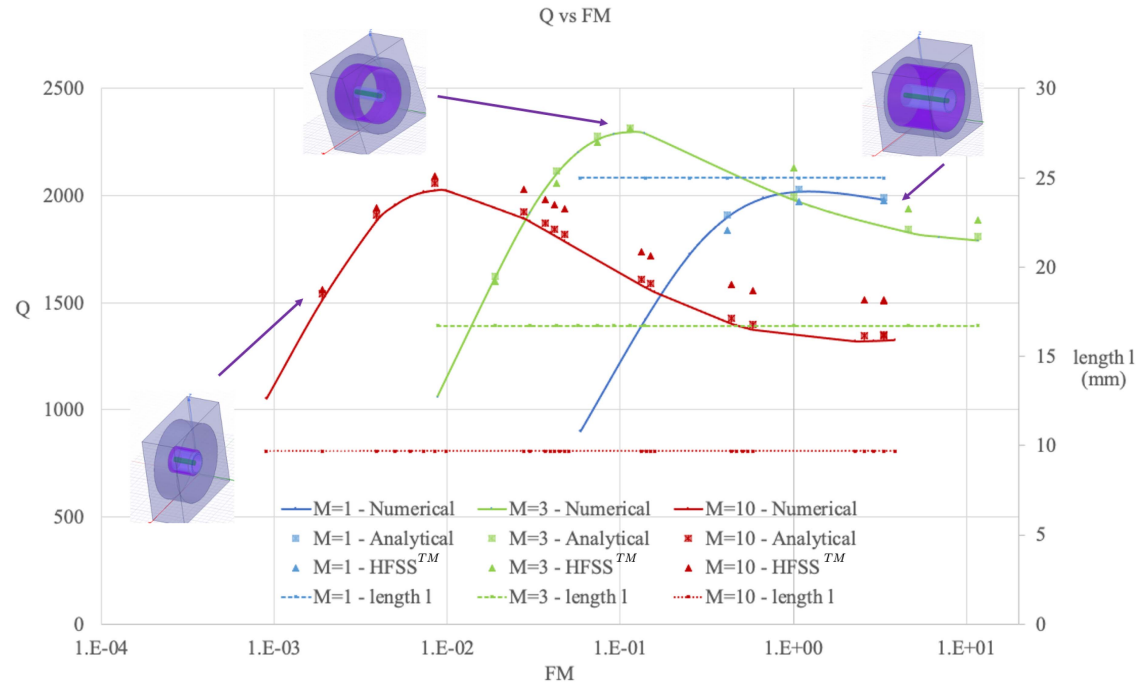

FIGURE 10. Quality factor vs. logarithm of factor FM for equivalent impedance ratios equal to 1, 3, and 10 for three-section coaxial SIRs at 1.5 GHz.

150 MHz (around 150 mm) than for those at 1.5 GHz (around 15 mm), which reduces the effects caused by discontinuities for the first ones. This illustrates the limitation of the model, which remains valid for topologies with very small lengths lc compared with the length l of the resonator. In the case of strong discontinuities, the model becomes more complex, making it necessary, for example, to take into account an additional transmission line at each discontinuity as shown in the study [11].

The study of these curves allows us to optimize the topology very quickly in terms of quality factor. Indeed, each curve makes it possible to identify the topology with the maximum

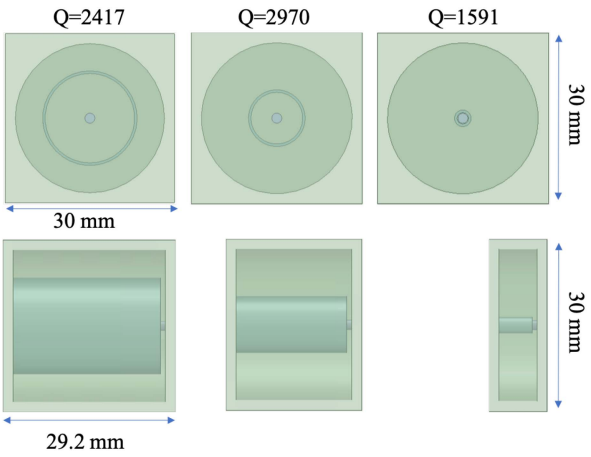

(a) Top and front views of two-section coaxial SIRs

(b) Top and front views of three-section coaxial SIRs

FIGURE 11. Quality factors (*HFSS*) and shape factors of two- and three-section coaxial SIRs at 1.5 GHz.

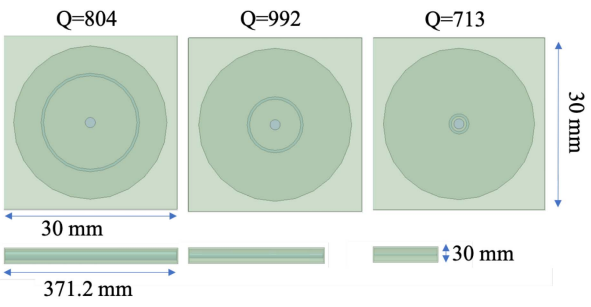

(a) Top and front views of two-section coaxial SIRs

(b) Top and front views of three-section coaxial SIRs

FIGURE 12. Quality factors (*HFSS*) and shape factors of two and three-section coaxial SIRs at 150 MHz.

quality factor, and those for a given fundamental frequency and external section width. Figs. 11 and 12 compare several geometries of two- and three-section resonators for frequencies of 1.5 GHz or 150 MHz. These figures indicate that the quality factor increases with the frequency. However, the comparison of topologies for the same frequency does not allow us to extract a trend of the quality factor in terms of the number of sections or length of the resonators. The use of an analytical model or numerical resolution makes it possible to immediately identify the maximum quality factor and corresponding topology for a fixed fundamental frequency and external section.

VI. CONCLUSION

In this paper, we have proposed a general method to calculate the quality factor of a quarter-wavelength n-section coaxial SIR. For filter design, knowledge of the quality factor of the resonators involved is an essential parameter to help evaluate the electrical performance that will be obtained. The procedure makes it possible to obtain an analytical model for the simplest cases, based on two or three sections. For a larger number of sections >3, a numerical resolution is possible. A comparison of different examples, notably at two different frequencies and with different sets of nested sections, mostly showed good agreement with results obtained in eigenmode with the *ANSYS HFSS* electromagnetic simulation tool. Indeed, for two and three sections, the relative error percentages do not exceed 11%. As the formalism is general, this method can be applied to structures with a higher number of nested sections, keeping in mind that discontinuity effects will impact the accuracy of the results. An important aspect of future work should be the integration of these effects into the models in order to push their limits when the number of sections increases.

REFERENCES

[1] I. Arregui et al., "High-power filter design in waveguide technology: Future generation of waveguide satellite filters in payloads handling increasing bit rates and numbers of channels," *IEEE Microw. Mag.*, vol. 21, no. 6, pp. 46–57, Jun. 2020.

[2] M. Yu, "Power-handling capability for RF filters," *IEEE Microw. Mag.*, vol. 8, no. 5, pp. 88–97, Oct. 2007.

[3] D. Sh-Asanjan and R. R. Mansour, "A novel coaxial resonator for high power applications," in *Proc. 44th Eur. Microw. Conf.*, 2014, pp. 295–298.
[4] P. Vizmuller, *RF Design Guide: Systems, Circuits, and Equations*. Norwood, MA, USA: Artech House, 1995.
[5] M. Sagawa, M. Makimoto, and S. Yamashita, "Geometrical structures and fundamental characteristics of microwave stepped-impedance resonators," *IEEE Trans. Microw. Theory Techn.*, vol. 45, no. 7, pp. 1078–1085, Jul. 1997.
[6] S. Yamashita and M. Makimoto, "The Q-factor of coaxial resonators partially loaded with high dielectric constant microwave ceramics," *IEEE Trans. Microw. Theory Techn.*, vol. 31, no. 6, pp. 485–488, Jun. 1983.
[7] M. Makimoto and S. Yamashita, *Microwave Resonators and Filters for Wireless Communication: Theory, Design and Application*, vol. 4. Berlin, Germany: Springer, 2001.
[8] G. B. Stracca and A. Panzeri, "Unloaded Q-factor of stepped-impedance resonators," *IEEE Trans. Microw. Theory Techn.*, vol. 34, no. 11, pp. 1214–1219, Nov. 1986.
[9] T. Yang, K. Ho, and G. M. Rebeiz, "Compact self-shielded 2–3 GHz high-Q coaxial fixed and tunable filters," *IEEE Trans. Microw. Theory Techn.*, vol. 62, no. 12, pp. 3370–3379, Dec. 2014.
[10] H. Aouidad, E. Rius, J.-F. Favennec, A. Manchec, and Y. Clavet, "UHF second order bandpass filters based on miniature two-section sir coaxial resonators," *Int. J. Microwaves Wireless Technol.*, vol. 8, no. 8, pp. 1187–1196, 2016.
[11] C. Hallet, J.-F. Favennec, E. Rius, J. Benedicto, L. Carpentier, and D. Pacaud, "Optimization of an air filled compact re-entrant coaxial resonator for a c-band bandpass filter," *IEEE Access*, vol. 6, pp. 54117–54125, 2018.
[12] J. Benedicto, H. Aouidad, E. Rius, J.-F. Favennec, A. Martin-Guennou, and A. Manchec, "Analytical modelling of three-section coaxial stepped impedance resonators for the design of compact tx bandpass filters," *IEEE Trans. Microw. Theory Techn.*, vol. 70, no. 9, pp. 4140–4155, Sep. 2022, doi: 10.1109/TMTT.2022.3194095.

JESSICA BENEDICTO (Member, IEEE) received the Ph.D. degree in physics from Blaise Pascal University, Clermont-Ferrand, France, in 2013. During her Ph.D. degree, she investigated the potential of metallodielectric multilayers, flat lenses with subwavelength resolution, and nonlocality in metals. In 2013, she held a postdoctoral position with Fresnel Institute, Marseille, France. The fields of application of her postdoctoral research were hybrid magnetic–electric dielectric scatterer near-field and far-field analyses. In 2015, she became an Assistant Professor with the University of Brest, Brest, France. She currently conducts research with the Laboratoire des Sciences et Techniques de l'Information, de la Communication et de la Connaissance (Lab-STICC), Brest, France. Her research focuses on the modeling and design of passive devices for microwave applications.

JEAN-FRANÇOIS FAVENNEC (Member, IEEE) received the Ph.D. degree in electronics from the University of Brest, Brest, France, in 1990, and the Accreditation to Supervise Research (HDR) in 2016. He became an Assistant Professor with the École Nationale d'Ingénieurs de Brest, Plouzané, France, in 1991. He mainly teaches electromagnetic theory and microwaves. He currently conducts research with the Laboratoire des Sciences et Techniques de l'Information, de la Communication et de la Connaissance (Lab-STICC), Brest, France. His research focuses on the modeling and design of passive devices for microwave applications and on filters.

ALEJANDRO BUITRAGO BERNAL was born in Bogotá, Colombia, in 1994. He received the B.Sc. and M.Sc. degrees in electronics engineering from the Universidad de los Andes, Bogotá, Colombia, in 2017 and 2019, respectively. He is currently working towards the Ph.D. in electronics engineering with the Lab-STICC Laboratory, Université de Bretagne Occidentale, Brest, France.

ERIC RIUS (Senior Member, IEEE) was the Vice-Head of the Laboratoire des Sciences et Techniques de l'Information, de la Communication et de la Connaissance (Lab-STICC), Brest, France, from 2016 to 2020. His research conducted with Lab-STICC concerns the design of passive microwave devices for centimetric and millimetric-wave applications. In 2013, he was appointed the European Microwave Lecturer by the European Microwave Association. He spent several months in Singapore as a Visiting Professor with Nanyang Technological University, Singapore. He is currently a Professor with the University of Brest, Brest, France. He is involved in many projects with the three French agencies, ANR, DGA, and CNES, and companies, such as Thales Alenia Space. He has supervised more than 23 Ph.D. students and several postdocs. He has participated in more than 110 Ph.D. and HDR defense juries. He has an H-score of 23, with more than 2300 citations overall. Dr. Rius was the TPC Chair of the 40th edition of the European Microwave Conference, which had more than 5000 attendees in 2010.